Received: 16 March 2021 | Revised: 24 May 2021 | Accepted: 18 June 2021

DOI: 10.1002/mp.15087

MEDICAL PHYSICS

RESEARCH ARTICLE

Stereotactic radiosurgery commissioning and QA test cases—A TG-119 approach for Stereotactic radiosurgery

Rebecca Culcasi[1] | **Geoffrey Baran**[1] | **Michael Dominello**[1,2] | **Jay Burmeister**[1,2]

[1]Karmanos Cancer Institute, Detroit, MI, USA

[2]Wayne State University School of Medicine, Detroit, MI, USA

Correspondence
Rebecca Culcasi, Karmanos Cancer Institute, Detroit, MI, USA.
Email: rebecca.culcasi@wayne.edu

Abstract

Purpose: To develop a standardized set of representative clinical treatment cases that pose a range of optimization problems for evaluating the plan quality and dosimetric accuracy within the commissioning process for linac-based stereotactic radiosurgery (SRS).

Methods: Five test cases with increasing complexity were created to validate delivery accuracy in SRS commissioning similar to the approach used by AAPM TG-119 in developing a test suite for IMRT commissioning. Standardized structure sets, planning goals, and delivery requirements were specified for each case including a small sphere target, irregular target, irregular target placed off-axis, multi-target, and abutting organs-at-risk (OARs). Various VMAT field arrangements including a single arc, two coplanar arcs, full arc and vertex half arc, and four noncoplanar arcs were tested to generate clinically appropriate treatment plans.

Results: The small spherical target was 1.0 cm in diameter. The irregular target was a clinical cavity (2.3 × 2.2 × 1.4 cm^3) and was shifted 4.5 cm for the irregular target off-axis case. The multi-target case used the irregular target and four spherical targets representing metastases ranging 0.9 to 1.6 cm in diameter, placed up to 7.5 cm off-axis. The abutting OARs case included an acoustic neuroma and target placed near the optic nerve. All spherical targets received 24 Gy and the cavity received 18 Gy. The abutting OAR cases included a 3.74 cc lesion adjacent to the brainstem receiving 13 Gy and a 1.11 cc lesion adjacent to the optic nerve receiving 12 Gy. All plans used a single-isocenter placed at the target center or geometric center of multiple targets. Planning goals for all cases included constraints for the target and brain minus PTV, along with brainstem and optic nerve where applicable. Deliverability was assessed through ion chamber measurements, in addition to composite and per-field planar measurements on Gafchromic film and small-field diode array. A mean and SD for measured versus planned doses of 101.0% ± 2.9% was observed over the 14 ion chamber measurements. Mean and SD for gamma pass rates were 98.5% ± 2.2% and 97.1% ± 4.9% for film and diode array, respectively, for gamma criteria of 2% and 1 mm.

Conclusion: These cases could provide the preliminary groundwork for a novel benchmark for institutions to evaluate linac-based SRS commissioning and delivery accuracy prior to clinical implementation. The rapid widespread implementation of linac-based SRS, the complexity associated with dosimetry and delivery, and high-profile treatment deviations that have already resulted from its use, highlight the importance of such a benchmark test suite. Comprehensive dosimetric measurements from this standardized set of SRS optimization problems were used to fine-tune and understand the limitations of our SRS planning and delivery system and establish a set of baseline data for comparison with other delivery platforms.

KEYWORDS
commissioning, stereotactic radiosurgery

1 | INTRODUCTION

Stereotactic radiosurgery (SRS) uses external beams of ionizing radiation to deliver ablative doses in commonly one, but up to five fractions, with stereotactic guidance and a localization accuracy of approximately 1 mm.[1–8] Due to the high demands for accurate and precise delivery, SRS has historically been delivered on dedicated and specialized equipment. Use of a linear accelerator for SRS was limited in the 1980s to a few academic centers, but recently there has been a paradigm shift to conventional linear accelerators being adapted or installed as multi-purpose machines capable of delivering SRS treatments.[9,10] Not only have technological advancements allowed for the progression to linac-based SRS delivery with circular aperture cone techniques, but also more complex MLC-based deliveries are being increasingly utilized.[11] Recent advances have also been achieved in treatment planning system (TPS) dose calculation accuracy and optimization for SRS. As the treatment of multiple brain metastases with SRS becomes more common, single-isocenter, multiple target linac-based approaches are being increasingly utilized to decrease treatment time.[12–20] Given the aforementioned dramatic increase in the use of linac-based SRS and the associated planning and delivery complexity, a standardized multi-institutional approach for testing and evaluating the accuracy and precision of these treatments would be of tremendous benefit.

Currently, institutions implementing SRS into their clinic are establishing institutional protocols for commissioning and following generic guidelines offered by the American Association of Physicists in Medicine (AAPM) task group (TG) reports, AAPM Medical Physics Practice Guidelines, and the American College of Radiology-American Society for Radiation Oncology (ACR-ASTRO) Practice Parameters. Common TG reports utilized for commissioning processes do not provide sufficient information for SRS applications. For example, TG-42 covers the SRS process from commissioning to delivery but was published in 1995, prior to the development of complex SRS technologies used today such as on-board imaging, MLCs, specialized equipment for small-field measurement, motion tracking software, and more.[1] While TG-142 provides recommended QA tolerances for specialized treatments, TG-106, covering accelerator beam data commissioning equipment and procedures, explicitly states that SRS remains beyond the scope of the report.[21–23] Recently, initial discussion regarding SRS commissioning was addressed in AAPM Medical Physics Practice Guideline 9a for SRS-SBRT but this document provides only a general discussion.[24] Even if sufficient guidance documentation were available for SRS commissioning, a set of standardized tests would be extremely valuable to provide a benchmark for such a complex technique. The AAPM TG-119 report was conceived to address a similar issue, the widespread implementation of IMRT without sufficient guidance and standardized benchmark tests. Concern regarding the relatively low pass rates on credentialing tests for IMRT spurred the development of the benchmark tests provided in TG-119 and these have been tremendously useful to the profession. A similar situation currently exists with the rapid proliferation of complex MLC-based linac-SRS delivery applied to small fields and nonequilibrium conditions, multiple targets treated with a single-isocenter, and substantially more complex delivery considerations. While the Imaging and Radiation Oncology Core (IROC) provides independent validation testing, the passing criteria for SRS anthropomorphic phantoms only requires TLD/OSLD agreement within 5% and gamma pass rates above 85% for 5% dose difference and 3 mm distance-to-agreement. These standards would be deemed unacceptable for SRS delivery accuracy for a patient plan. Moreover, of the 211 linac irradiations performed during 2013–2016 from institutions

participating in NCI sponsored SRS clinical trials, only 79% passed these criteria, compared to a passing rate of 96% when using Gamma Knife.[25] These results demonstrate a substantial fraction of facilities failing to meet tolerances that are relatively lenient compared to typical clinical SRS planning and delivery requirements and indicate additional challenges in accurately commissioning linacs for SRS compared to dedicated SRS equipment. Following commissioning, IROC phantoms are commonly utilized for end-to-end testing of the clinical SRS procedures. If such stringent precision and accuracy are deemed necessary for such a specialized treatment, the lenient passing criteria and poor passing rates for IROC credentialing tests are quite concerning. An additional concern is that the IROC test case for the SRS head phantom is limited to a simple spherical target volume, which is substantially less complex and clinically meaningful than would be a real representative clinical case. As such, a set of standardized test cases with realistic targets, goals, and tolerances for the implementation and QA of such complex delivery would be particularly valuable.

With the increased demand for extremely accurate and conformal dose distributions shaped around the target volumes treated with SRS, in addition to the technological advancements in treatment planning and delivery systems that make this possible, SRS commissioning has become extremely complex and challenging. We propose a standardized approach to SRS commissioning through the use of a set of representative clinical treatment cases that pose a range of optimization problems for evaluating the plan quality and dosimetric accuracy within the commissioning process for linac-based SRS. These cases could provide the preliminary groundwork for what could be a novel benchmark for institutions to evaluate linac-based SRS commissioning and delivery accuracy, a similar approach to the "standard" test cases that were established in TG-119 for IMRT commissioning. The rapid widespread implementation of SRS technique, complexity associated with dosimetry and delivery, and high-profile treatment deviations that have already resulted from its use, highlight the importance of such a benchmark test suite.

2 | MATERIALS AND METHODS

2.1 | Test suite: Planning conditions and measurement specifications

A set of standardized test cases were established for commissioning and evaluating an SRS program. These tests increase in complexity starting with a simple spherical target at the central axis to a complex clinical scenario treating off-axis targets including an acoustic neuroma abutting the brainstem and lesion abutting the optic nerve. These varying degrees of complexity serve to fully test the mechanical capabilities of the delivery process. The DICOM-RT data consisting of CT images of the anthropomorphic RANDO male phantom as an equivalent to a human head and structure sets can be imported by the user to create and optimize VMAT plans for the various cases. VMAT plans were created with the orientations shown in Figure 1, including (A) a single arc, (B) two coplanar arcs, (C) full arc and vertex

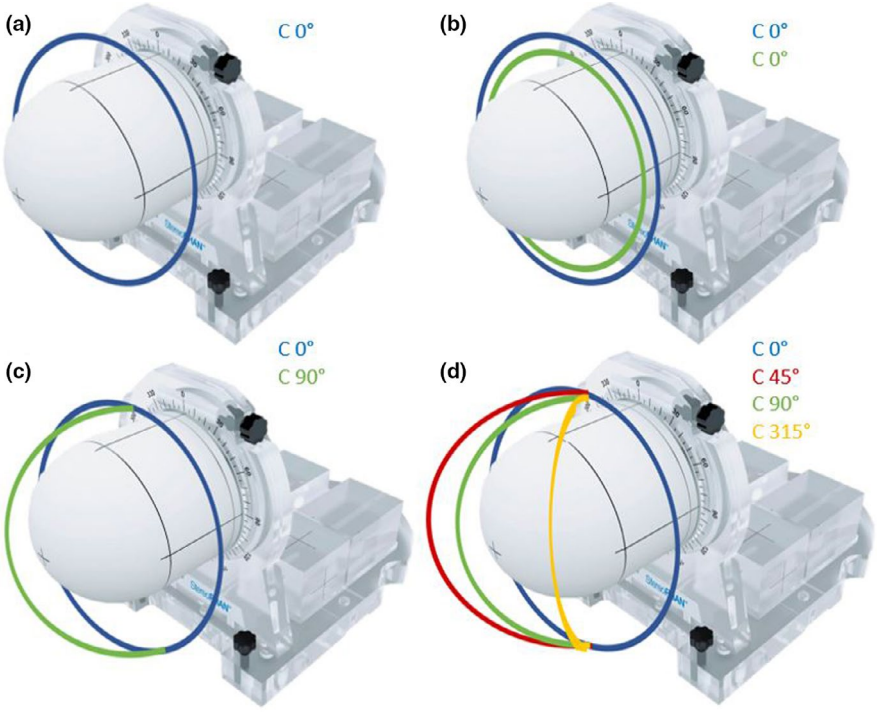

FIGURE 1 VMAT arc orientations utilized for test suite cases. These will be referred to throughout the paper as orientations a, b, c, and d, respectively

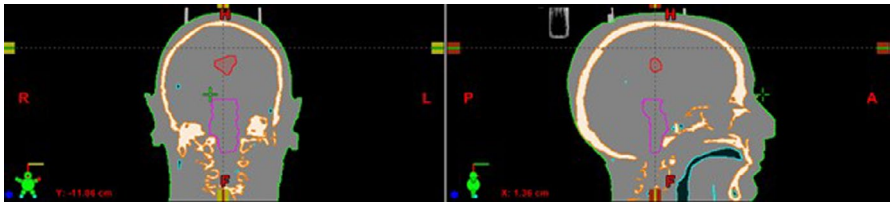

FIGURE 2 Irregular target structure: Coronal and sagittal views of the centrally located 2.3 × 2.2 × 1.4 cm^3 cavity

half arc, and (D) four noncoplanar arcs with 0, 45, 315, and 90/270 degree couch angles based on the UAB technique.[17] The planning goals during optimization are stated for each of the cases. These tests were all planned and delivered using 6 MV in our institution but should be planned using the energy that will be utilized locally. Verification plans were calculated and measured using equipment specified in Sections 2.2–2.4.

2.1.1 | Test 1: Small spherical target

The small sphere case consists of a single spherical target of 1.0 cm diameter placed at the center of the brain within the RANDO cranial CT set. VMAT plans were created for orientations A–D from Figure 1 with the isocenter placed at the center of the target meeting the following goals: $V_{100\%}$ > 99% of the 24 Gy prescription for the target, and $V_{12\ Gy}$ < 5 cc and $V_{10\ Gy}$ < 10 cc for the brain minus PTV. An ion chamber and coronal planar dose measurements were made for the target at the isocenter.

2.1.2 | Test 2: Irregular target

The resection cavity of a patient who underwent SRS treatment was transferred to the RANDO cranial CT set (Figure 2) to provide a centrally located, irregularly shaped target. The irregular target case consists of a clinical cavity of dimensions 2.3 cm × 2.2 cm × 1.4 cm placed near the center of the brain. VMAT plans were created for orientations B and C from Figure 1 with the isocenter placed at the center of the target meeting the following goals: $V_{100\%}$ > 99% of the 18 Gy prescription for the target, and $V_{12\ Gy}$ < 5 cc and $V_{10\ Gy}$ < 10 cc for the brain minus PTV. An ion chamber and coronal planar dose measurements were made for the target at the isocenter.

2.1.3 | Test 3: Irregular target off-axis

The target shape in Test 3 was identical to the previous test except that it was translated 4.5 cm off-axis. VMAT plans were created for orientations B–D from Figure 1 with the isocenter placed centrally in the brain at the location of the irregular target case. The planning goals for the target remain the same as the previous case. An ion chamber and coronal planar dose measurements were made for the target off-axis from the isocenter. For the 4-arc plan (orientation D), per-field ion chamber and planar dose measurements were made in addition to the composite measurements.

2.1.4 | Test 4: Multi-target

The multi-target case was created on the RANDO cranial CT set (Figure 3) with the intent of representing a patient with multiple metastases throughout the brain. The case consisted of the clinical resection cavity from the irregular target case placed 1.3 cm off-axis, a 0.9-cm diameter sphere placed 7.5 cm off-axis, a 1.5-cm sphere placed 3.7 cm off-axis, a 1.2-cm sphere placed 2.9 cm off-axis, and a 1.6-cm sphere placed 4.5 cm off-axis. All spherical metastases received a prescription dose of 24 Gy and the cavity received a prescription of 18 Gy. The details for each target are presented in Table 1. VMAT plans were created for orientations B and D from Figure 1 with a single-isocenter placed at the geometric center of the targets meeting the following goals: $V_{100\%}$ > 99% of each of the targets, and V_{12} < 5 cc and V_{10} < 10 cc for the brain minus PTV. For each of the targets, per-field and composite ion chamber and planar dose measurements were made.

2.1.5 | Test 5: Abutting oars

The acoustic neuroma target contours for a patient who underwent SRS treatment were transferred to the RANDO cranial CT set (Figure 4) to provide a complex target near a critical organ-at-risk (OAR). To increase the complexity of the abutting OAR case, an additional target was placed near the optic nerve, to provide the additional challenge of planning and delivery for a multi-target single-isocenter technique. The abutting OARs case consisted of a 3.74 cc lesion (2.4 cm × 1.5 cm × 2.0 cm) representing an acoustic neuroma against the brainstem and a 1.11 cc lesion (1.9 cm × 0.9 cm × 1.3 cm) against the optic nerve. The lesion by the brainstem was prescribed 13 Gy and the lesion by the optic nerve was prescribed 12 Gy. VMAT plans were created for orientations B and C from Figure 1 with the isocenter placed at the geometric center of the targets meeting the following goals:

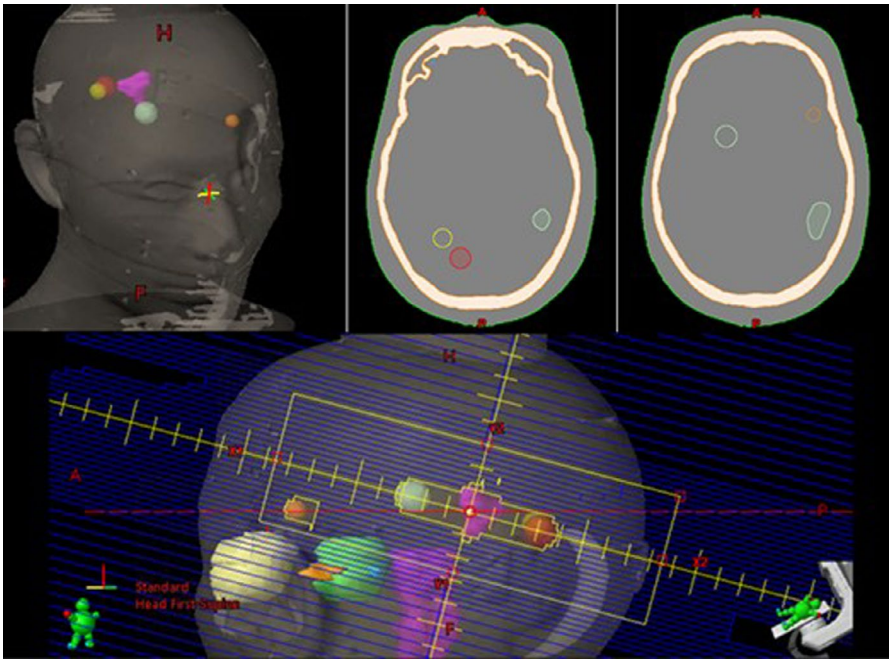

FIGURE 3 Multi-target structures: 3D representation and coronal views of the centrally located 2.3 × 2.2 × 1.4 cm^3 cavity in addition to the four spherical metastases. The beams eye view representation is shown to depict the collimator angle chosen to maintain use of the HD-MLCs throughout the duration of the arc

TABLE 1 Multi-target structures: Volume, dimensions, off-axis placement and prescription of each of the structures included in the case

	Cavity	Met 1	Met 2	Met 3	Met 4
Volume (cc)	2.81	0.43	1.67	0.81	2.01
Dimensions	2.3 × 2.2 × 1.4 cm^3	0.9 cm sphere	1.5 cm sphere	1.2 cm sphere	1.6 cm sphere
Distance from isocenter (cm)	1.3	7.5	3.7	2.9	4.5
Prescription	18 Gy	24 Gy	24 Gy	24 Gy	24 Gy

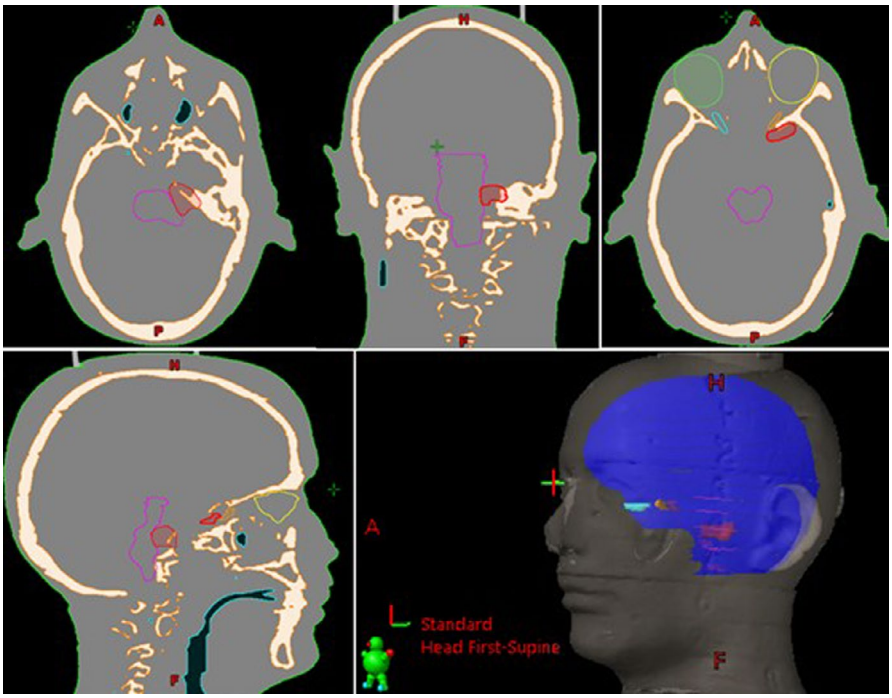

FIGURE 4 Axial, coronal, and sagittal views, in addition to the 3D representation of the lesions abutting brainstem and optic nerve

$V_{100\%}$ > 99% for each of the targets, V_{12} < 5 cc and V_{10} < 10 cc for the brain minus PTV, D_{max} < 15 Gy and V_{10} < 0.5 cc for the brainstem, and D_{max} < 10–12 Gy and V_8 < 0.2 cc for the optic nerve. For each of the targets and abutting OARs, per-field ion chamber were made, along with a per-field and composite planar

dose measurement consisting of the gradient region between the target and OAR.

2.2 | Equipment

Ideally, the phantom utilized for SRS commissioning should have "head-like" spherical or cylindrical geometry and be made of water-equivalent material that allows for point measurements (e.g., ionization chamber) and planar dose measurements (e.g., film or array). Figure 5a shows an example of such a phantom. The phantom should be scanned with the appropriate head/brain CT protocol expected to be used clinically for SRS cases, with slice thickness ideally equal to or <1 mm. Downloaded CT datasets developed from this study and planned in the user's treatment planning system should be re-calculated on the phantom, similar to patient quality assurance measurements.

For this study, all end-to-end commissioning measurements utilized Sun Nuclear Corporation's StereoPHAN phantom with the A16 ion chamber insert (Figure 5b), coronal film plane insert (Figure 5c), and SRS MapCHECK small-field diode array insert (Figure 5d). The StereoPHAN was placed on a lockbar for reproducible positioning. Prior to use, the precision leveling knobs were used to level the StereoPHAN base and the cylinder was oriented at 0 or 90 degrees depending on the insert being used. A CBCT was acquired of the StereoPHAN to verify the phantom set up each day prior to taking measurements. While StereoPHAN was utilized for this study, any "head-like" phantom with the ability to perform point and planar dose measurements would be acceptable for SRS commissioning.

All treatment plans were optimized and calculated in Eclipse treatment planning system v.11.0.31 (Varian Medical Systems), the progressive resolution optimizer (PRO) algorithm was used for optimization during VMAT planning and the anisotropic analytical algorithm (AAA) was used for dose calculation. The calculation grid size was set to the finest resolution at 0.1 cm.

2.3 | Chamber measurements

The cylindrical ionization chambers used for SRS commissioning point measurements should follow the small-field dosimetry recommendations from the IAEA Technical Reports Series No. 483 code of practice such that the chamber volume is between 0.002 and 0.13 cm^3.[26] Examples of acceptable ionization chambers include but are not limited to, IBA's CC04, Standard Imaging's Exradin A16 or A26, or PTW's PinPoint ion chamber. All chamber measurements should be made with the clinically used geometries for couch, gantry and collimator rotation. Chamber measurements should be taken in both the target and a nearby low dose avoidance structures routinely encountered clinically including brainstem and optic nerve. For our measurements, Standard Imaging's Exradin Model A16 chamber, with collection volume of 0.007 cm^3 was used for all point measurements.

Conversion of the chamber reading to dose was done by irradiating the phantom with an AP-PA parallel-opposed isocentric 4 × 4 cm^2 field to reduce the effects of daily variations in linac output. Prior to acquiring point measurements on a given day, the calibration plan was delivered to obtain a conversion factor by assuming the dose was correctly calculated by the planning system for the 4 × 4 cm^2 field. An intermediate field size of 4 × 4 cm^2 is used as a compromise toward approaching small-field conditions while minimizing any large-field or small-field correction factors for microionization chambers.

2.4 | Composite and per-field planar measurements

All tests required at least one coronal plane measurement with fields irradiating the phantom with the planned couch, collimator, and gantry angles. Composite planar dose measurements involved irradiating a piece of Gafchromic EBT-XD film (Ashland Materials) placed at the center of each lesion. Gafchromic EBT-XD film is optimal for SRS applications given its useful dose range of 0.4–40 Gy. Per-field and composite planar

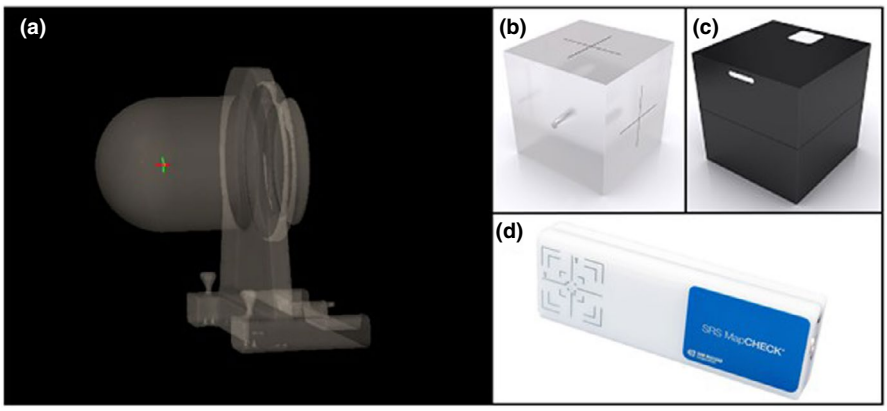

FIGURE 5 (a) Sun Nuclear's StereoPHAN phantom utilized for end-to-end commissioning measurements in this study with the corresponding (b) A16 ion chamber insert, (c) coronal film plane insert, and (d) SRS MapCHECK small-field diode array insert

dose distributions during irradiation of the phantom with the planned couch, collimator, and gantry angles were also measured with Sun Nuclear Corporation's SRS MapCHECK small-field diode array which consisted of a 77 × 77 mm^2 array, with 0.48 × 0.48 mm^2 active measurement area in the diodes making it compliant with AAPM TG-101 recommendations, that can measure field sizes as small as 5 mm.[3,27]

Dose distributions were analyzed using gamma criteria of 3%/1 mm, 2%/2 mm, and 1%/1 mm for dose and distance to agreement (DTA), respectively, as AAPM TG-218 recommends a tighter tolerance for SRS than the standard 3% dose and 2 mm DTA for IMRT. A threshold value of 10% of the maximum dose was used to avoid including gamma statistics from regions of very low dose.[27–29] Film analysis can be performed in any software capable of performing gamma analysis.[28] The green channel was utilized for film analysis to produce the most accurate results for the dose delivered, as this channel has been proven to have high sensitivity and low uncertainty in the dose range suitable for SRS commissioning.[30] This study used RIT software (Radiological Imaging Technology Inc) for film analysis. SNC patient software (Sun Nuclear Corporation) was used for SRS MapCHECK analysis to maintain errors in the analysis to <2% since it corrects measurements based on output factor, pulse repetition rate, diode temperature response, and angular dependence.[27]

3 | RESULTS

3.1 | Planning results

The planning statistics for each of the five test cases, including both targets and respective relevant OARs are summarized in Tables 2–6.

The intent of this study was to meet the clinical goals outlined and ultimately test the accuracy of the delivery capabilities of the system through these plans, not to create the best plan possible. As such, the plan quality metrics are not intended to serve as goals to be achieved.

3.2 | Delivery results

3.2.1 | Ion chamber measurements

All ion chamber results for the small sphere test were measured at isocenter. Measurements were performed on two separate days for each field for each treatment

TABLE 2 Treatment plan statistics for Test 1: "Small Spherical Target"

Planning parameter	Plan goal (cGy)	Orientation A	Orientation B	Orientation C	Orientation D
Target $V_{100\%}$	≥99%	99%	99%	99%	99%
Normal brain $V_{12\ Gy}$	<5 cc	2.18	2.25	2.04	2.02
Normal brain $V_{10\ Gy}$	<10 cc	3.27	3.34	2.92	2.84
Conformity Index		1.02	0.98	0.98	0.96
Gradient Index		5.74	6.07	5.57	5.67

TABLE 3 Treatment plan statistics for Test 2: "Irregular Target"

Planning parameter	Plan goal (cGy)	Orientation B	Orientation C
Target $V_{100\%}$	≥99%	99%	99%
Normal brain $V_{12\ Gy}$	<5 cc	4.01	3.82
Normal brain $V_{10\ Gy}$	<10 cc	6.93	6.26
Conformity Index		1.01	1.00
Gradient Index		4.31	3.90

TABLE 4 Treatment plan statistics for Test 3: "Irregular Target Off-Axis"

Planning parameter	Plan goal (cGy)	Orientation B	Orientation C	Orientation D
Target $V_{100\%}$	≥99%	99%	99%	99%
Normal brain V_{12Gy}	<5 cc	4.46	4.14	4.31
Normal brain V_{10Gy}	<10 cc	7.55	6.88	6.99
Conformity Index		1.01	1.02	1.02
Gradient Index		4.68	4.22	4.26

TABLE 5 Treatment plan statistics for Test 4: "Multi-target"

Planning parameter	Plan goal (cGy)	Orientation B	Orientation D
Cavity $V_{100\%}$	≥99%	99.77%	99.86%
Met 1 $V_{100\%}$	≥99%	99.00%	99.41%
Met 2 $V_{100\%}$	≥99%	99.79%	99.00%
Met 3 $V_{100\%}$	≥99%	99.90%	99.13%
Met 4 $V_{100\%}$	≥99%	99.83%	99.20%
Normal brain $V_{12\ Gy}$	<5 cc	36.79	21.47
Normal brain $V_{10\ Gy}$	<10 cc	82.38	37.13
Conformity Index	Cavity	1.10	1.19
	Met1	1.05	1.07
	Met2	1.06	1.01
	Met3	1.06	1.06
	Met4	1.05	1.01

TABLE 6 Treatment plan statistics for Test 5: "Abutting OARs"

Planning parameter	Plan goal (cGy)	Orientation B	Orientation C
AN $V_{100\%}$	≥99%	99.00%	99.00%
Target $V_{100\%}$	≥99%	99.68%	99.03%
Normal brain $V_{12\ Gy}$	<5 cc	0.86	0.85
Normal brain $V_{10\ Gy}$	<10 cc	2.53	2.30
Brainstem D_{max}	<15 Gy	12.14	13.38
Brainstem $V_{10\ Gy}$	<0.5 cc	0.24	0.15
Optic Nerve D_{max}	<10–12 Gy	9.61	8.73
Optic Nerve $V_{8\ Gy}$	<0.2 cc	0.01	0.00
Conformity Index	AN	1.20	1.21
	Target	1.41	1.48

technique (e.g., single arc, 4-field). Per- field measurements ranged from 98.1% to 101.8% of the predicted measurement, with a mean of 99.3%. Ion chamber measurements for the cavity test were measured for the coplanar treatment technique on two separate days. Per-field measurements ranged from 102.5% to 105.4% of the predicted, with a mean of 103.9%. Similarly, for the cavity off-axis test, per-field measurements ranged from 100.0% to 109.0% of the predicted, with a mean of 102.6% for all field orientations. For the single-isocenter multi-target test, ion chamber measurements were performed for each target, approximately at the center of the dose distribution. The per-field measurements for the targets ranged from 89.9% to 106.3% of the predicted, with a mean of 99.3% for all targets and all field orientations. Lastly, for the clinical case involving an acoustic neuroma abutting the brainstem and a target in close proximity to the optic nerve, ion chamber measurements ranged from 103.7% to 110.0% for the high-dose regions and 101.2%–138.9% for the low-dose regions. The 138.9% per-field measurement was for a very low-dose region contributing approximately 1% of the prescription dose. The targets had a mean of 105.9% of the predicted dose. Total planning doses for high-dose regions are presented in Table 7 for all test cases.

3.2.2 | Planar measurements

All planar dose results were measured with the target centered on the StereoPHAN insert and delivered at the appropriate couch, collimator, and gantry angles as planned. While the StereoPHAN software now has a function to maximize the number of off-isocenter targets captured in a plan delivery, this was not available for our measurements. Measurements were performed only once for each treatment plan. Per-field measurements were made for the SRS MapCHECK and are shown in parentheses in Table 8. All composite films had gamma pass rates >93.4% for 3%/1 and 2%/1 mm. Excluding the multi-target cavity and met 4 using the 2%/1 mm gamma criteria, all composite SRS MapCHECK measurements had gamma pass results >96.8% for both gamma criteria. The large outlier observed in the per-field gamma pass rate range for

TABLE 7 Ion chamber results summarized

Case	Field orientation	Target	Avg. meas./ TPS (%)	Per-field range (%)
Small spherical target	A	Sphere	99.2	98.9–99.5
	B	Sphere	98.8	98.4–99.3
	C	Sphere	99.8	99.0–101.8
	D	Sphere	98.9	98.1–101.0
Irregular target	B	Cavity	103.9	102.5–105.4
Irregular target off-axis	B	Cavity	101.8	100.0–103.5
	D	Cavity	103.4	101.1–109.0
Multi-target	D	Cavity	98.5	95.3–106.2
		Met 1	97.0	89.9–101.5
		Met 2	100.0	94.6–103.5
		Met 3	98.2	94.8–99.8
		Met 4	102.7	99.8–106.3
Abutting OARs	C	AN/BS	106.4	104.4–110.0
		Target/ ON	105.4	103.7–106.7
Average			101.0%	
Standard deviation			2.9%	
95% confidence limit			6.7% (4.6%[a])	

[a]If you exclude last 2 measurements where we believe to have pushed the limits of the machine.

TABLE 8 Planar dose (film and diode array) results summarized

Case	Field orientation	Target	Film gamma pass rate		SRS MapCHECK gamma pass rate	
			2%/1 mm	3%/1 mm	2%/1 mm	3%/1 mm
Small spherical target	A	Sphere	100.0%	100.0%	100.0%	100.0%
	B	Sphere	100.0%	100.0%	100.0%	100.0%
	C	Sphere	100.0%	100.0%	100% (99.3–100%)	100.0%
	D	Sphere	100.0%	100.0%	100% (99.3–100%)	100.0%
Irregular target	B	Cavity	99.8%	100.0%	98.3% (97.7–99.1%)	99.4% (98.8–99.4%)
Irregular target off-axis	B	Cavity	100.0%	100.0%	100.0% (97.6–99.7%)	100.0% (99.2–100.0%)
	D	Cavity	99.9%	100.0%	96.8% (94.0–97.4%)	97.7% (96.5–98.7%)
Multi-target	D	Cavity	97.5%	99.4%	85.4% (59.9–99.4%)	98.8% (74.8–100.0%)
		Met 1	100.0%	100.0%	97.8% (69.8–99.5%)	100.0% (87.5–100.0%)
		Met 2	98.9%	100.0%	99.4% (86.3–100.0%)	100.0% (95.4–100.0%)
		Met 3	93.4%	98.4%	97.1% (76.9–99.7%)	100.0% (97.9–100.0%)
		Met 4	97.9%	99.7%	86.2% (4.9–98.6%)	99.7% (5.1–100%)
Abutting OARs	C	AN/BS	96.1%	97.1%	99.2% (96.4–99.5%)	99.5% (99.4–99.5%)
		Target/ ON	95.0%	100.0%	99.5% (95.3–98.9%)	99.7% (98.1–99.5%)
Average			98.5%	99.6%	97.1%	99.6%
Standard deviation			2.2%	0.9%	4.9%	0.7%
95% confidence limit			94.2%	98.0%	87.5%	98.3%

multi-target met 4 resulted from a field that only contributed approximately 5% of the target dose. Composite film measurements resulted in 95% CLs of 98.0% and 94.2%, for 3%/1 and 2%/1 mm, respectively. Composite SRS MapCHECK measurements resulted in 95% CLs of 98.3% and 87.5%, for 3%/1 and 2%/1 mm, respectively. The per-field measurements showed substantially more variation in passing results. Low individual per-field passing rates occurred for complex multi-arc arrangements where some fields contribute a low

fraction of the total dose delivered and require further planning system optimization. Excluding the lowest contributor, which was observed to be for met 4 arc 2, the per-field SRS MapCHECK measurements resulted in an average of 97.4% ± 7.3% and 93.4% ± 11.9%.

4 | DISCUSSION

We have performed comprehensive dosimetric measurements on a standardized set of SRS optimization problems to establish CLs and to fine-tune and understand the limitations of our SRS planning and delivery system. An extensive list of end-to-end planning and delivery scenarios was considered in the creation of VMAT arc orientations for the test suite cases. While one might not choose to test all of these scenarios when commissioning an SRS system, we chose to evaluate the entire set to determine which tests were ultimately most useful. This set consisted of the 14 scenarios (combinations of target configurations and delivery orientations) listed in Tables 2–6. After evaluation of the planning results and in an effort to optimize the utility of these cases to evaluate planning and delivery capabilities while minimizing the planning and delivery time, we chose to reduce this to nine scenarios for delivery as shown in Tables 7 and 8.

Starting with Test 1: Small spherical target, all four VMAT arc orientations from Figure 1 were created to test their utility in evaluating our planning and delivery capabilities. After delivering all of these scenarios, the single arc and two coplanar arcs were deemed equivalent in assessing the planning and delivery capabilities and we leave it to the user to decide which version to use to assess the coplanar delivery. The major consideration when deciding which of these VMAT arc scenarios to use is the gantry speed. In the subsequent cases, a single arc scenario was often omitted due to the very slow gantry speed required to deliver the high number of MU and complex motion with the use of jaw tracking. The exception was Test 5: Abutting OARs due to the lower prescriptions used for those targets and the smaller number of MUs needed. Test 2: Irregular target was planned with two coplanar and two noncoplanar arcs, but the coplanar arcs plan was deemed sufficient based on the planning statistics. When transitioning to Test 3: Irregular target off-axis, two coplanar arcs and both noncoplanar orientations were evaluated for planning. Since ultimately many institutions utilize a four noncoplanar arc orientation to maximize normal brain sparing, the two noncoplanar arcs were omitted for the delivery phase. Further consideration with additional targets in the multi-target case involved the two coplanar arc orientation and the four noncoplanar arcs, due to the ability to spare the normal brain. However, the coplanar arc orientation resulted in high normal brain doses that relegated this plan clinically unacceptable, and only the noncoplanar arcs were delivered. This plan was representative of a clinical scenario in which dose bridging between targets would be likely to occur requiring the planner to push the TPS to prevent this from occurring and attempt to minimize the dose between targets. Due to the close proximity of the clinical lesions, the two coplanar arcs and simple noncoplanar arcs were both deemed sufficient for plan quality, but the non-coplanar was utilized for delivery.

From the delivered plans, confidence limits were established to provide information to fine-tune and understand the limitations of our SRS planning and delivery system. Confidence limits were calculated using $CL = |\mu| + 1.96\sigma$. All plans were calculated with the AAA algorithm. As with TG-119, the purpose of this study was not to create optimal plan results, but rather to test how well the measured doses compare to those predicted by the planning system. The purpose of stating the plan results in terms of the planning statistics and the MU is to allow other institutions to create comparable plans with similar modulation and complexity.

It is important to have an understanding of the uncertainties involved in dose measurement for small-field SRS treatments. In the planning and dose calculation of the plan, there are uncertainties in the measured values versus TPS calculations dependent upon the segmentation resolution and calculation grid size. In the measurement itself, there are uncertainties in the small-field size output factor modeled in the TPS that is highly dependent upon the detector used, correction factors applied to the chamber readings, detector positioning, and jaw and MLC uncertainty.[26,31] During the delivery, there are uncertainties inherent in the machine capabilities based on the tolerance limits for the couch, gantry, and collimator angle, in addition to the positioning for jaw tracking, isocenter, and much more. All of these need to be considered when evaluating the results.

Overall, the average measured A16 reading to TPS value ratio was 101.0% ± 2.6%. Excellent planar composite dosimetry results were obtained, with gamma pass rates >93% for all targets within all delivery scenarios using a gamma criteria of 3%/1 mm.

Point measurements were acquired in locations such that dose gradients across the chamber could be minimized. The goal was to place the chamber in regions where the gradient was <5% throughout the contoured chamber volume. It is important to consider that there are various uncertainties that remain when acquiring point measurements such as the uncertainty in the correction factors used for the ion chamber, the calculation grid size that is used for the plan, and the visualization on CBCT for localizing the chamber. Plans were calculated with the smallest grid size allowable by the TPS in order to have the most accurate representation of the dose delivered to the small chamber volume. The small sphere chamber measurements

were consistently low, which requires further investigation as the jaw size is approximately 1.2 cm and small-field complications could be the cause of this and an output correction factor could account for the discrepancy. We attempted to minimize the uncertainty of the A16 point measurement on CT by contouring a small high-resolution segment, using the mean dose delivered to the volume as the expected "point" dose, and minimizing the variation between the minimum and maximum dose within the contoured volume to <5% whenever possible. In certain situations with high dose gradients, this was not possible, as was seen for met 4 in the multi-target case for arcs 1 and 4, and for the clinical case for the acoustic neuroma, optic nerve, and the target abutting the optic nerve. It was noted that the A16 measurements for the four noncoplanar arcs orientation that were outside of the 5% chamber reading tolerance for the irregular target off-axis and multi-target cases were for fields with lower contributions to the point of interest, having only approximately 23% contribution to the total dose. While the target and optic nerve chamber measurements for Test 5: Abutting OARs differed from the TPS calculated values by more than 5%, this was not unexpected given that these measurements were performed in a very high local gradient. The results from the ionization chamber measurements should be used to modify beam parameters such that there is greater agreement between the planned and measured doses. Future work should involve a multi-institutional study to establish standard achievable confidence limits.

The results shown in this report represent the initial commissioning results for a Varian TrueBeam linac using 6 MV with an HD-MLC and without refinement of small-field output factors, focal spot size, DLG, and transmission factor. As was seen in some of the A16, film, and SRS MapCHECK measurements during the commissioning process, fine-tuning of the machine is necessary to further optimize the treatment planning system for SRS scenarios. No external validation has been performed up to this point for SRS. The results show that these structure sets and the resulting plan complexities are sensitive enough to identify the limitations in the TPS and delivery systems. This standardized approach to linac-based SRS commissioning provides the potential foundation for a mechanism for the medical physics community to evaluate the implementation and delivery accuracy of SRS systems.

5 | CONCLUSION

This work establishes a standardized approach to SRS commissioning through the creation of a set of representative clinical treatment cases that pose a range of optimization problems for evaluating the plan quality and dosimetric accuracy within the commissioning process for linac-based SRS. The standardized structure sets, planning goals, and delivery requirements were specified for each of the cases including a small sphere target, irregular target, irregular target placed off-axis, multi-target, and abutting targets. Planning results and delivery results using multiple dosimetric techniques are provided as a benchmark for users of this test suite. The rapid widespread implementation of this SRS technique, complexity associated with dosimetry and delivery, and high-profile treatment deviations that have already resulted from its use, highlight the importance of such a benchmark test suite. The cases presented here provide preliminary groundwork for what could be a novel benchmark for institutions to evaluate their linac-based SRS program prior to clinical implementation as we intend to obtain multi-institutional collaborative involvement for our future work, similar to the approach provided by AAPM TG-119 for IMRT commissioning with a standardized test suite.

CONFLICT OF INTEREST

The authors have no relevant conflicts of interest to disclose.

DATA AVAILABILITY STATEMENT

Research data are not shared.

REFERENCES

1. Schell M, Bova F, Larson D, et al. *AAPM report no 54 stereotactic radiosurgery American Institute of Physics Inc*. Woodbury; 1995.
2. Wen N, Li H, Song K, et al. Characteristics of a novel treatment system for linear accelerator–based stereotactic radiosurgery. *J Appl Clin Med Phys*. 2015;16(4):125-148.
3. Benedict SH, Yenice KM, Followill D, et al. Stereotactic body radiation therapy: the report of AAPM Task Group 101. *Med Phys*. 2010;37(8):4078-4101.
4. Winston KR, Lutz W. Linear accelerator as a neurosurgical tool for stereotactic radiosurgery. *Neurosurgery*. 1988;22(3):454-464.
5. Rahimian J, Chen JC, Rao AA, Girvigian MR, Miller MJ, Greathouse HE. Geometrical accuracy of the Novalis stereotactic radiosurgery system for trigeminal neuralgia. *J Neurosurg*. 2004;101(Supplement3):351-355.
6. Grimm J, Grimm SYL, Das IJ, et al. A quality assurance method with submillimeter accuracy for stereotactic linear accelerators. *J Appl Clin Med Phys*. 2011;12(1):182-198.
7. Kim J, Wen N, Jin JY, et al. Clinical commissioning and use of the Novalis Tx linear accelerator for SRS and SBRT. *J Appl Clin Med Phys*. 2012;13(3):124-151.
8. Denton TR, Shields LB, Howe JN, Spalding AC. Quantifying isocenter measurements to establish clinically meaningful thresholds. *J Appl Clin Med Phys*. 2015;16(2):175-188.
9. Dhabaan A, Elder E, Schreibmann E, et al. Dosimetric performance of the new high-definition multileaf collimator for intracranial stereotactic radiosurgery. *J Appl Clin Med Phys*. 2010;11(3):197-211.
10. Dimitriadis A. *Assessing the dosimetric and geometric accuracy of stereotactic radiosurgery*. University of Surrey (United Kingdom); 2016.
11. Tanyi J, Kato C, Chen Y, Chen Z, Fuss M. Impact of the high-definition multileaf collimator on linear accelerator-based

intracranial stereotactic radiosurgery. *Br J Radiol*. 2011;84(1003):629-638.
12. Clark GM, Popple RA, Young PE, Fiveash JB. Feasibility of single-isocenter volumetric modulated arc radiosurgery for treatment of multiple brain metastases. *Int J Radiat Oncol Biol Phys*. 2010;76(1):296-302.
13. Wolff HA, Wagner DM, Christiansen H, Hess CF, Vorwerk H. Single fraction radiosurgery using Rapid Arc for treatment of intracranial targets. *Radiat Oncol*. 2010;5(1):1-8.
14. Huang Y, Zhao B, Chetty IJ, Brown S, Gordon J, Wen N. Targeting accuracy of image-guided radiosurgery for intracranial lesions: a comparison across multiple linear accelerator platforms. *Technol Cancer Res Treat*. 2016;15(2):243-248.
15. Kim S, Tseng T-C, Morrow A. Spatial variations of multiple off-axial targets for a single isocenter SRS treatment in Novalis Tx linac system. *J Radiosurg SBRT*. 2015;3(4):287.
16. Ezzell GA. The spatial accuracy of two frameless, linear accelerator-based systems for single-isocenter, multitarget cranial radiosurgery. *J Appl Clin Med Phys*. 2017;18(2):37-43.
17. Clark GM, Popple RA, Prendergast BM, et al. Plan quality and treatment planning technique for single isocenter cranial radiosurgery with volumetric modulated arc therapy. *Pract Radiat Oncol*. 2012;2(4):306-313.
18. Huang Y, Chin K, Robbins JR, et al. Radiosurgery of multiple brain metastases with single-isocenter dynamic conformal arcs (SIDCA). *Radiother Oncol*. 2014;112(1):128-132.
19. Thomas EM, Popple RA, Wu X, et al. Comparison of plan quality and delivery time between volumetric arc therapy (RapidArc) and Gamma Knife radiosurgery for multiple cranial metastases. *Neurosurgery*. 2014;75(4):409-418.
20. Thomas A, Niebanck M, Juang T, Wang Z, Oldham M. A comprehensive investigation of the accuracy and reproducibility of a multitarget single isocenter VMAT radiosurgery technique. *Med Phys*. 2013;40(12):121725.
21. Kutcher GJ, Coia L, Gillin M, et al. Comprehensive QA for radiation oncology: report of AAPM radiation therapy committee task group 40. *Med Phys*. 1994;21(4):581-618.
22. Klein EE, Hanley J, Bayouth J, et al. Task Group 142 report: quality assurance of medical acceleratorsa. *Med Phys*. 2009;36(9Part1):4197-4212.
23. Das IJ, Cheng CW, Watts RJ, et al. Accelerator beam data commissioning equipment and procedures: report of the TG-106 of the Therapy Physics Committee of the AAPM. *Med Phys*. 2008;35(9):4186-4215.
24. Halvorsen PH, Cirino E, Das IJ, et al. AAPM-RSS medical physics practice guideline 9. a. for SRS-SBRT. *J Appl Clin Med Phys*. 2017;18(5):10-21.
25. Molineu A, Hernandez N, Nguyen T, Ibbott G, Followill D. Credentialing results from IMRT irradiations of an anthropomorphic head and neck phantom. *Med Phys*. 2013;40(2):022101.
26. Cranmer-Sargison G. Dosimetry of small static fields used in external beam radiotherapy: a review of IAEA TRS 483. *J Med Phys*. 2018;43(suppl. 1):1.
27. Rose MS, Tirpak L, Van Casteren K, et al. Multi-institution validation of a new high spatial resolution diode array for SRS and SBRT plan pretreatment quality assurance. *Med Phys*. 2020;47(7):3153-3164.
28. Low DA, Harms WB, Mutic S, Purdy JA. A technique for the quantitative evaluation of dose distributions. *Med Phys*. 1998;25(5):656-661.
29. Miften M, Olch A, Mihailidis D, et al. Tolerance limits and methodologies for IMRT measurement-based verification QA: recommendations of AAPM Task Group No. 218. *Med Phys*. 2018;45(4):e53-e83.
30. Wen N, Lu S, Kim J, et al. Precise film dosimetry for stereotactic radiosurgery and stereotactic body radiotherapy quality assurance using Gafchromic™ EBT3 films. *Radiat Oncol*. 2016;11(1):1-11.
31. Alfonso R, Andreo P, Capote R, et al. A new formalism for reference dosimetry of small and nonstandard fields. *Med Phys*. 2008;35(11):5179-5186.

How to cite this article: Culcasi R, Baran G, Dominello M, Burmeister J. Stereotactic radiosurgery commissioning and QA test cases—A TG-119 approach for Stereotactic radiosurgery. *Med. Phys*. 2021;00:1–12. https://doi.org/10.1002/mp.15087